ARTICLE

Richard Cseh · Michael Hetzer · Kristina Wolf
Jürgen Kraus · Gerhard Bringmann · Roland Benz

Interaction of phloretin with membranes: on the mode of action of phloretin at the water-lipid interface

Abstract The interaction of phloretin with single lipid bilayers on a spherical support and with multilamellar vesicles was studied by differential scanning calorimetry (DSC) and nuclear magnetic resonance (NMR). The results indicated that phloretin interacts with the lipid layer and changes its structural parameters. In DSC experiments, phloretin in its neutral form strongly decreased the lipid phase transition temperature and slightly reduced the cooperativity of the phase transition within the lipid layer. In NMR measurements, phloretin led to an increase of the transverse relaxation time constant but had no effect on the spin-lattice relaxation time constant. The overall dipole moment of phloretin was experimentally determined and was found to be roughly 40% lower than has been published previously. This result suggested that the size of the dipole moment of phloretin does not provide such a high contribution to the effect of phloretin on the dipole potential of monolayers and bilayers as has been published previously. To understand the discrepancy between phloretin adsorption and dipole potential change, we performed computational conformational analysis of phloretin in the gas phase. The results showed that a wide distribution of the dipole moments of phloretin conformers exists, which mainly depends on the orientation of the OH moieties. The adsorption of phloretin as determined from its binding to solid supported bilayers differed from the one determined from dipole potential measurements on black lipid membranes. The difference between the phloretin dissociation constants of both types of experiments suggested a change of its dipole moment normal to the membrane surface in a concentration-dependent manner, which was in agreement with the results of the computational conformational analysis.

Introduction

The effects of phloretin (Fig. 1) on natural and artificial membranes deal in most cases with changes of the conductance for ions and the permeability for a number of neutral solutes (Forman et al. 1982; Gunn et al. 1975; Jennings and Solomon 1976; LeFevre and Marshall 1959; Macey and Farmer 1970; Owen 1974; Toon and Solomon 1987; Verkman and Solomon 1982). These changes are mainly attributed to the phloretin-induced change of dipole potential of the membranes. Phloretin in its neutral form decreases the dipole potential of membranes and lipid monolayers by the introduction of dipoles aligned opposite to those of the lipid molecules (Andersen et al. 1976; Cousin and Motais 1978, Cseh and Benz 1998; Melnik et al. 1977; Reyes et al. 1983).

Besides the electric effects discussed in the literature in detail, phloretin should also affect structural parameters of lipid membranes. Owing to the ability of

R. Cseh · R. Benz (✉)
Lehrstuhl für Biotechnologie, Theodor-Boveri-Institut
(Biozentrum) der Universität Würzburg,
97074 Würzburg, Germany
e-mail: roland.benz@mail.uni-wuerzburg.de

M. Hetzer
Lehrstuhl für Experimentelle Physik V der
Universität Würzburg, Würzburg, Germany

K. Wolf · J. Kraus · G. Bringmann
Lehrstuhl für Organische Chemie der Universität Würzburg,
Würzburg, Germany
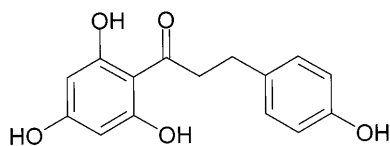
Fig. 1 Structural formula of phloretin [3-(4 hydroxyphenyl)-1-(2,4,6-trihydroxyphenyl)-1-propanone]

phloretin to adsorb to membranes and lipid monolayers, a strong influence on structural properties, in particular on lipid packing and phase transition, can be expected as the effects of hydrophobic interactions between lipids and phloretin. Of further interest is the examination of the structure of the phloretin molecule with respect to the possible variation of its conformers and their dipole moments, since the dipole potential reducing effect of phloretin is mainly attributed to its large dipole moment (Andersen et al. 1976; Cseh and Benz 1998; Reyes et al. 1983). The phloretin effect on structural properties of membranes and monolayers, together with results of electric measurements, should permit a much better understanding of the interaction of phloretin with membranes.

In this study we investigated the effects of phloretin on structural properties of lipid membranes using different methods. Information about the phloretin-mediated change of molecular order of lipid layers was gained by differential scanning calorimetry (DSC). DSC is well established as a method to study phase transition temperature, excess enthalpy and cooperativity of lipid bilayers and multilamellar lipid vesicles (MLVs) (Biltonen and Lichtenberg 1993; McElhaney 1982; Naumann et al. 1992). Interaction of MLVs with surface active substances such as phloretin may cause changes of the phase transition temperature. According to an increase/decrease of the phase transition temperature and the change of the shapes of the heat capacity curves, it is possible to estimate the quality and quantity of the lipid-phloretin interaction.

Spherical supported unilamellar lipid vesicles (SSVs) were used to directly measure the physical parameters of phloretin adsorption in a quantitative way. Adsorption of phloretin, often determined only by the phloretin-induced dipole potential change (Cseh and Benz 1998; De Levie et al. 1979; Reyes et al. 1983), can also be gained by this method and provides additional information about the saturation behavior of phloretin on membranes. We determined the characteristic adsorption parameters on the basis of a Langmuir adsorption isotherm. By comparison with the adsorption isotherm determined by measurements of the dipole potential change (Cseh and Benz 1998; De Levie et al. 1979; Reyes et al. 1983), we obtained information on whether phloretin adsorption is accompanied by possible structural changes and dipole rearrangements.

In another set of experimental conditions we employed deuterium NMR spectroscopy (^{2}H NMR) to obtain structural and dynamic information about the effect of phloretin adsorption to a lipid bilayer. ^{2}H NMR relaxation experiments were performed on SSVs, which allowed us to estimate whether phloretin changes the lateral diffusion of lipid molecules (Bayerl and Bloom 1990).

Up to now, virtually no attention has been paid to possible variations of phloretin conformations and their dipole moments as a result of external forces. Especially the variation of the dipole moment may drastically affect the phloretin-induced dipole potential at the lipid-water interface. A contribution to that issue is given by a computer-supported conformational analysis of phloretin and its possible dipole moments. These calculations, on the basis of energetic minimization, provided conformers of the molecule in the gas phase and additional information about the probability of their occurrence on the basis of a Boltzman weighting. Based on these conformers we included also solvation effects in the semiempirical calculations. We were able to determine the dipole moments of these phloretin conformations and to calculate the resulting dipole moment and its direction with respect to the structure of the molecule. These theoretically obtained data supported the experimental results concerning the interpretation of the molecular interaction of phloretin with membranes.

Materials and methods

Materials

Dimyristoylphosphatidylcholine (DMPC) and headgroup-deuterated dimyristoylphosphatidylcholine (DMPC-d_{13}) were obtained from Avanti Polar Lipids (Alabaster, Ala., USA). Phloretin was obtained from Sigma (St. Louis, Mo., USA). Benzene was spectroscopically pure and ethanol was analytical grade (Merck, Darmstadt, Germany). Ultrapure water was obtained by passing deionized water through Milli-Q equipment (Millipore, Bedford, Mass., USA). For the SSVs used in ^{2}H NMR measurements, silica beads of the highest purity with a radius of 200 $\pm$ 50 nm were used as the solid support. The SSVs used for the measurement of phloretin adsorption were a commercially available kit (Transil, Nimbus, Leipzig, Germany). The diameter of the silica beads was normally 30 μm. The beads were non-covalently coated with egg phosphatidylcholine (egg-PC), with a surface area extent of 10 m^2/g beads.

Buffers and solutions

In DSC experiments, the samples were prepared by dissolving pure lipid (DMPC) or a mixture of lipid and phloretin in a mixture of benzene and ethanol (1:1 v/v). After evaporation of the solvent in vacuum (12 h), the samples were incubated with buffer (0.1 M NaCl and 20 mM NaH$_2$PO$_4$) at a temperature well over the phase

transition temperature and vortexed until a homogeneous emulsion was obtained. The lipid concentration of the DSC samples was 1.5 mg/ml buffer. The phloretin concentration was 50 mol% of the lipid. In DSC experiments the pH of the buffer was adjusted to 5, 7, and 9. In adsorption experiments, phloretin was dissolved in 1 M NaOH and added to buffer (0.1 M NaCl and 20 mM NaH_2PO_4) for final concentrations between 10 μM and 0.3 mM. The pH was adjusted to 5.5. SSVs were prepared by the vesicle fusion technique described in detail elsewhere (Bayerl and Bloom 1990; Naumann et al. 1992). For the lipid/phloretin SSVs a lipid/phloretin solution (pH 7) was used, of which the preparation was analogous to the DSC measurements. Adsorption experiments were performed at 22 °C, NMR experiments at 30 °C.

Differential scanning calorimetry

High-sensitivity DSC measurements were performed with a MC-2 microcalorimeter (MicroCal, North Hampton, Ma., USA). The calorimeter was interfaced to a personal computer and the data acquisition was controlled by this device. The scans for all measurements were done within a temperature range of 5–40 °C, at a scan rate of 30 °C/h and a 12 s time increment (filter constant). No significant differences in the DSC endotherms were observed for heating and cooling mode scans except for a small hysteresis. Data analysis was performed using the MicroCal Origin DSC analysis software package. Within the data analysis we standardized the raw data by baseline substraction (Bayerl et al. 1988; Jacobson and Papahadjopoulos 1975; Kodama et al. 1982; Lohner et al. 1987).

Measurement of phloretin adsorption

Silica beads coated with egg-PC bilayer were incubated in buffer containing various concentrations of phloretin. The lipid concentration was 0.18 mM. The beads were separated by centrifugation for 5 min at 10,000g. Phloretin concentrations before incubation and after separation of the beads were determined by UV spectroscopy at a wavelength of 285 nm using a Perkin-Elmer Lambda 2 UV/VIS spectrometer (Perkin-Elmer, Norwalk, Conn., USA). The linearity of the absorption units versus aqueous phloretin concentration was verified. Adsorption of phloretin was determined as the difference between its concentration in buffer before incubation and after separation of the beads and converted into molar ratios of phloretin adsorbed to lipid. The stability of the lipid layer on the silica beads in the presence and absence of phloretin was controlled by UV spectroscopy at a wavelength of 285 nm. We found detached lipid in suspension; however, its concentration was extremely small compared to the concentration of the lipid attached to the beads.

^{2}H NMR measurements of SSVs

^{2}H NMR measurements were performed at 76.7 MHz using a Bruker AMX 500 spectrometer equipped with a Bruker broadband high-power probe with a 10 mm sample coil. A quadrupolar echo sequence with a CYCLOPS phase cycling scheme was used and the pulse length for a 90° pulse was 5.5 μs. The repetition time was 300 ms and 2048 complex data points were collected in quadrature with a dwell time of 5 μs. The spectra were obtained by a one-dimensional Fourier transform starting at the top of the quadrupolar echo. The pulse spacing of the ^{2}H NMR spectra was 35 μs.

Longitudinal relaxation time T_{1z} measurements were performed by employing the inversion recovery pulse sequence and the T_{1z} values were obtained by analysis of the area of the spectra. For transverse quadrupolar echo relaxation time (T_{2e}) measurements, the pulse spacing times τ of the quadrupolar echo sequence were varied between 160 and 760 μs and semilogarithmic plots of the peak echo intensity versus 2τ yielded linear dependencies of slope $(T_{2e})^{-1}$. The calculation of the oriented ^{2}H NMR spectra (bilayer normal parallel to the external magnetic field $\boldsymbol{B}_0$) was achieved by using an interactive de-pake-ing program (Sternin et al. 1983). The residual second moment M_{2r} was calculated numerically from the corresponding spectrum $f(\omega)$ according to the equation:

$$M_{2r} = \frac{\int_{-\infty}^{\infty} (\omega - \omega_0)^2 f(\omega)\, d\omega}{\int_{-\infty}^{\infty} f(\omega)\, d\omega} \tag{1}$$

Computational methods

The semiempirical AM1 (Dewar et al. 1985) and PM3 (Stewart 1989) calculations for the gas phase as well as the AM1/SM5.2 calculations for solvent effects were performed on Silicon Graphics INDIGO (R4000) workstations using the VAMP 6.1 program (Rauhut et al. 1998) and the program AMSOL (Hawkins et al. 1997), starting from geometries preoptimized by the TRIPOS force field as implemented within the SYBYL (1999) program package. The conformational space of phloretin was searched semiempirically by varying the corresponding dihedral angles of the aliphatic chain and of the OH moieties and by the calculation of reaction coordinates using the corresponding keywords of the VAMP program package. For all conformers, geometry optimizations were done by applying the EF algorithm with a gradient norm specification of 0.1 mdyn/Å. The results of the AM1 gas phase calculations were taken as input geometries for the AMSOL program using the solvation model SM5.2 (solvent: water) and the default optimization algorithm implemented herein. The gradient norm was specified as 0.45 kcal/Å. The ab initio calculations (6-31G* basis set) were performed on the Fujitsu VPP700 supercomputer of the Leibniz Rechenzentrum in Munich using the Gaussian94 program package (Frisch et al. 1995).

Results

DSC with multilamellar lipid vesicles

DSC evaluation of lipid vesicles is highly sensitive to impurities and contaminations of the lipid and is therefore a suitable method to determine the interaction of phloretin with lipid in bilayers and multilayers. Figure 2 shows DSC scans of DMPC MLVs in the absence (A) and in the presence of 50 mol% phloretin (B). Pure MLVs exhibited a main phase transition temperature, T_m, of 23.6 °C which is strictly independent of aqueous pH. Pretransition, which is due to the transition from gel to rippled phase (Lee 1977), occurred at 13.5 °C. Any impurity which interferes with the packing of the lipid reduces T_m (Biltonen and Lichtenberg 1993). Under the influence of phloretin, T_m is clearly reduced to 13 °C at pH 5 (dashed line in Fig. 2B), which indicates reduction of the lipid order, i.e., the entropy of the lipid is increased.
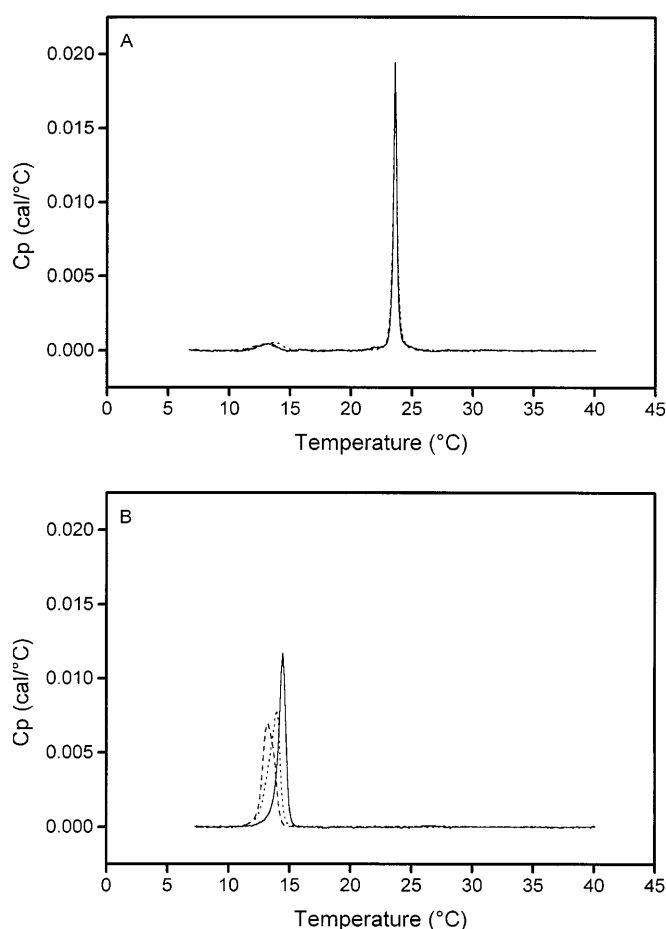
Fig. 2 DSC endotherms (excess heat capacity C_p versus temperature) of multilamellar DMPC lipid vesicles in the absence (**A**) and in the presence (**B**) of 50 mol% (of the lipid) phloretin at pH 5 (*dashed lines*), pH 7 (*dotted lines*) and pH 9 (*full lines*). The DSC scans were recorded in the heating mode. The curves of the scans in the absence of phloretin are almost identical, which means that they appear as a single line in **A**. All curves are baseline corrected

This effect appeared to be pH dependent with a larger decrease of T_m the lower the pH. At pH 7 (dotted line in Fig. 2B) the phase transition temperature was 14 °C, whereas T_m was about 14.5 °C at pH 9 (solid line in Fig. 2B). This result is in agreement with earlier findings that only the neutral form of phloretin changes the properties of lipid monolayers and membranes (Andersen et al. 1976, Cseh and Benz 1998; LeFevre and Marshall 1959). The pretransition at 13.5 °C disappeared at a very small phloretin concentration of less than 1 mol% (pH 5) where the main transition was only a little affected. This result indicated that the pretransition was indeed more sensitive to phloretin-induced lipid pertubation.

It is noteworthy that the variation within the pH range 5–9 caused a smaller effect on T_m than would be expected bearing in mind that the concentration of neutral phloretin in water showed a drastic change in this pH range. At pH 5, nearly all the phloretin molecules are neutral whereas only about 2% of the phloretin remains undissociated at pH 9 (pK_a = 7.35, Reyes et al. 1983). In contrast to this, the difference between T_m at pH 5 and pH 9 was much smaller than that between pH 9 and the reference without phloretin. This result indicated that the effect of the phloretin on the lipid phase transition was already near the maximum at pH 9 even though only a small amount was in the neutral form. The results of the DSC measurements are summarized in Table 1. They clearly show that the phase transition temperature of pure DMPC was pH independent. The addition of phloretin did not only change the phase transition temperature but also led to an increase of the width at half-height, $T_{1/2}$, which is related to the purity of the system and the cooperativity of the phase transition. The broadening of the endotherms appeared also to be somewhat pH dependent, although we could not observe a systematic change. Bechinger and Seelig (1991) and Verkman and Solomon (1982) pointed out that phloretin has a high affinity to membranes; it partitions to a high degree to membranes without destabilizing the bilayer structure. The results of the DSC measurements derived from the experiments described here confirmed this. In spite of the comparatively strong decrease of lipid order indicated by the strong decrease of the phase transition temperature in

Table 1 Parameters calculated from the heat capacity-temperature data of the DSC measurements with DMPC multilamellar lipid vesicles in the presence (+) and in the absence (−) of 50 mol% phloretin at pH 5, 7, and 9. Phase transition temperature T_m and the width at half-height $T_{1/2}$ are the means ± SD of at least five measurements

PH	± phloretin	T_m (°C)	$T_{1/2}$ (°C)
5	−	23.6 ± 0.04	0.39 ± 0.001
5	+	13.0 ± 0.20	1.33 ± 0.210
7	−	23.6 ± 0.06	0.34 ± 0.098
7	+	14.0 ± 0.14	1.25 ± 0.210
9	−	23.6 ± 0.06	0.32 ± 0.075
9	+	14.4 ± 0.03	0.61 ± 0.074

the presence of phloretin, the endotherms still showed relatively sharp peaks with moderate broadening. A much larger effect on the broadening of the endotherms has been reported from DSC measurements with similarly high doses of compounds mixed with the lipids such as cholesterol (Linseisen et al. 1993) and myelin basic protein (Reinl and Bayerl 1993). Phloretin appears therefore as a molecule, which adsorbs to a high degree to membranes but only slightly affects cooperativity of the lipids. Dehydration of the lipid head groups caused by phloretin adsorption, as has been proposed previously (Bechinger and Seelig 1991), cannot be excluded here but is presumably not the only effect of lipid-phloretin interaction because of the strong decrease of the phase transition temperature, T_m. Dehydration of lipids is usually accompanied by an increase of the phase transition temperature (Cevec et al. 1981; Heise et al. 1991; Kodama et al. 1982; Kurrle et al. 1990). It is noteworthy that the endotherms of the DSC measurements in the presence of phloretin are nearly symmetric. An asymmetry would represent an indication of either gel or liquid-crystalline region preference of the component integrated in the lipid layer (Ben-Yashar et al. 1987; van Osdol et al. 1992). Obviously phloretin does not exhibit any distribution preference to a certain phase state, which is an important result when its adsorption to different surfaces is considered. It is noteworty that phloretin in its neutral form integrates also into monolayers and decreases the phase transition temperature (Cseh and Benz 1999).

Computational calculation of the phloretin conformers

The semiempirical conformational analysis using the AM1 parametrization yielded the most stable conformations of the carbon skeleton 1A–1D (Fig. 3). Except for the OH moiety next to the carbonyl group, which takes its stable arrangement by forming a hydrogen bond with the carbonyl oxygen, additional conformers are generated by rotating the OH groups about the adjacent C-O single bond. For these three hydroxy
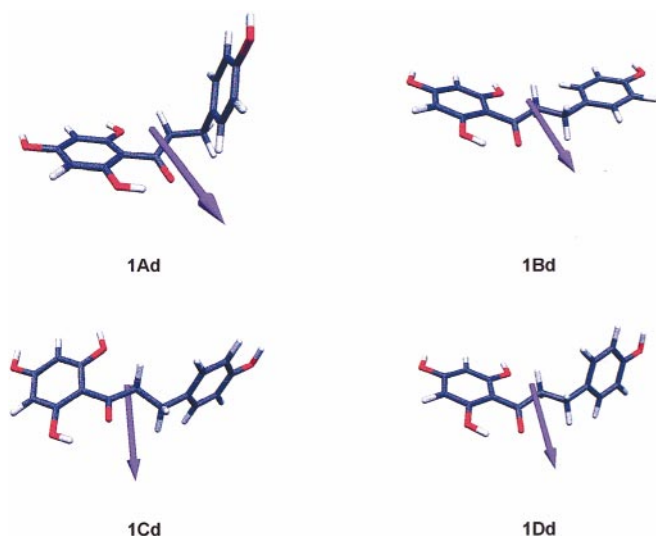
Fig. 3 Phloretin conformers in the gas phase as calculated by the semiempirical AM1 parametrization. Each of the conformers 1Ad–1Dd represents an example of the basic conformations of the ketonic form. The *arrows* indicate the dipole moment vectors; their lengths are proportional to the corresponding calculated dipole moments
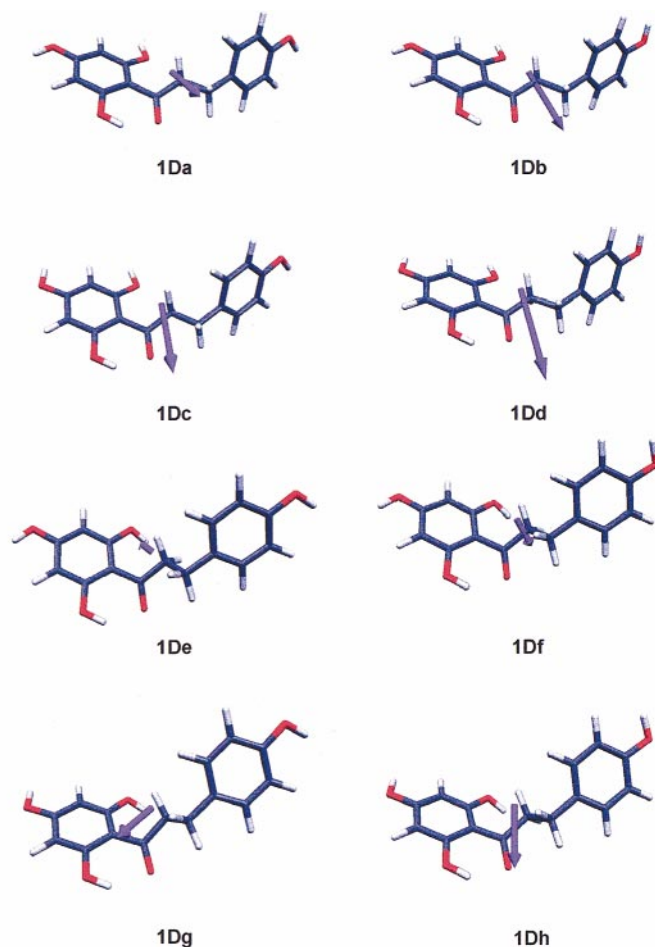
Fig. 4 Phloretin conformers in the gas phase as calculated by the semiempirical AM1 parametrization. The basic conformer 1D is shown in all stable arrangements a–h. The *arrows* indicate the dipole moment vectors; their lengths are proportional to the corresponding calculated dipole moments

functions, two minimum geometries were found, being the two possible arrangements in plane with the aromatic ring stabilized by hydrogen bonds between the oxygen atom and the aromatic hydrogens. Consequently, taking into account the orientations of the OH groups, each of the basic conformations 1A–1D split up into $2^3 = 8$ conformers, denoted as a–h (Fig. 4). By semiempirical geometry optimization, all eight arrangements a–h with different heats of formations were found for the conformers 1A, 1C, and 1D (Table 2). In contrast, the basic geometry 1B remained stable only for the orientations a–d. The interaction of the flexible OH group in the *ortho* position to the carbonyl function with the methylene moiety of the aliphatic chain, as found in the conformations e–h, obviously disturbed the nearly planar arrangement of the two aromatic rings in geometry 1B. Therefore, the total number of conformers found was 28 (instead of 32).

The dipole moments of the 28 conformers calculated with the AM1 parametrization vary over a wide range from 0.75 to 5.8 D, which mainly depends on the orientation of the OH moieties. These values were subjected to a Boltzmann weighting based on the relative energies (heats of formation), H_f°, of the conformers according to the equation:

$$\frac{N}{N_0} = \exp\left(-\frac{\Delta\Delta H_f^\circ \times 4.1868 \times 10^3}{N_A k_B T}\right) \qquad (2)$$

in which k_B is the Boltzman constant and T the temperature (295 K). The calculated contributions N/N_0 of the discrete conformers N relative to the absolute minimum conformer N_0 ($=1Da$) were normalized. By multiplication with the calculated dipole moments μ, the contribution to μ_{tot} of each conformer was obtained. Summation of these weighted contributions gave the overall dipole moment μ_{tot} of phloretin. The results of the AM1 parametrization are summarized in Table 2. The calculated value of 3.25 D lies in the same order of magnitude as the calculated value found by Andersen et al. (1976), but is distinctly smaller by 40%. These calculations describe the properties of an isolated molecule in the gas phase. Interactions with solvent molecules, possibly stabilizing conformers bearing higher dipole moments, have been neglected. Switching to the PM3 parametrization (which is known to calculate electronic effects improperly) tended to calculate smaller discrete dipole moments and the Boltzmann-weighted value of 2.9 D is even lower than the result of the AM1 calculations.

The possible tautomerization of phloretin (1) to the enols 2 and 3 was taken into account by calculations on the conformers 2Da and 3Da (Table 2). The initial geometries of these molecules were generated from the absolute minimum conformer 1Da of the non-enolized phloretin (1). The AM1-calculated relative heats of formation of 2Da and 3Da are 13.2 and 18 kcal/mol

Table 2 Computational calculation of the relative heat of formation H_f° and dipole moment μ of the conformers of phloretin in the gas phase using the semiempirical AM1 parametrization. The conformer with lowest heat of formation (1Da) was defined to $H_f^\circ = 0$; the others were normalized to this. Based on the four stable conformations of the carbon skeleton 1A–1D, rotation of the OH groups gave the conformers 1Aa–1Ah, 1Ba–1Bd, 1Ca–1Ch, and 1Da–1Dh of the ketonic form. The calculation of the enolic forms 2Da and 3Da was based on the starting geometries of 1Da. The table also shows the contribution by Boltzmann statistics and the corresponding contribution to the total dipole moment μ_{tot}. For details, refer to the text

Conformer	rel. H_f° (kcal/mol)	Contribution by Boltzmann statistics [%]	μ (D)	Contribution to μ_{tot} (D)
1Aa	0.629	4.815	2.354	0.113
1Ab	0.730	4.060	3.760	0.153
1Ac	1.368	1.382	3.969	0.055
1Ad	1.513	1.082	5.796	0.063
1Ae	3.014	0.086	0.822	7.053×10^{-4}
1Af	3.062	0.079	1.769	1.400×10^{-3}
1Ag	3.167	0.066	1.902	1.260×10^{-3}
1Ah	3.283	0.054	3.912	2.131×10^{-3}
1Ba	0.663	4.546	1.696	0.077
1Bb	0.720	4.129	3.830	0.158
1Bc	0.413	6.934	3.351	0.232
1Bd	1.495	1.116	5.401	0.060
1Ca	0.012	13.65	3.109	0.424
1Cb	0.023	13.40	2.878	0.386
1Cc	0.744	3.965	4.483	0.178
1Cd	0.762	3.846	4.691	0.180
1Ce	2.255	0.309	1.780	5.502×10^{-3}
1Cf	2.270	0.301	0.750	2.260×10^{-3}
1Cg	2.379	0.251	2.896	7.261×10^{-3}
1Ch	2.397	0.243	2.812	6.839×10^{-3}
1Da	0.000	13.92	2.329	0.324
1Db	0.047	12.86	3.432	0.442
1Dc	0.734	4.033	4.242	0.171
1Dd	0.787	3.867	4.843	0.179
1De	2.226	0.325	0.842	2.733×10^{-3}
1Df	2.221	0.327	1.659	5.431×10^{-4}
1Dg	2.352	0.262	2.567	6.736×10^{-3}
1Dh	2.364	0.257	3.098	7.966×10^{-3}
1				$= \mu_{tot} = 3.245$
2Da	13.20	3.381×10^{-11}	5.314	0.000
3Da	18.00	1.026×10^{-14}	4.172	0.000

(55.6 and 75.8 kJ/mol, respectively) higher than that of the non-enolized molecule 1Da. PM3 values of 14.9 and 21.7 kcal (62.7 and 91.4 kJ/mol, respectively) show the same tendency. When Boltzmann weighted, owing to their high energy content, the contribution of the enols 2 and 3 to the overall dipole moment is negligibly small. Consequently, no complete conformational analysis of the enols was carried out as the missing conformers were expected to be even more unstable.

To verify the higher energy contents of the enols, ab initio calculations using the RHF method and the 6-31G* basis set were carried out (no dipole moments were calculated as this method neglects electron correlation). The resulting energetic separation of 14.58 and 24 kcal/mol (61.4 and 101 kJ/mol, respectively) for 2Da and 3Da confirms the semiempirical results and thus the instability of these tautomers compared with 1Da. We additionally performed semiempirical AM1-AMSOL calculations in order to estimate solvent effects. The conformers 1Aa–1Dh and the enols 2Da and 3Da of the AM1 calculations were taken as the starting geometries for the program AMSOL. The implemented method generates a continuous space bearing the electrostatic properties of the chosen solvent around the input molecule, followed by the calculation of the energy of the molecule embedded in this solvent shell. Depending on the solvent, the order of the relative energies of different conformations may change, thus indicating (de)stabilization due to solvent effects.

Determination of the dipole moment of phloretin

Water as a polar and protic solvent was also chosen for our calculations. Compared with the results for the gas phase, some of the conformers with higher dipole moments were slightly stabilized by the calculated influence of water. Consequently, the overall Boltzmann-weighted dipole moment of phloretin increased to 4.7 D. Since these values of the dipole moment of phloretin differed by 40% from the published calculated value (5.6 D; Andersen et al. 1976), we determined the dipole moment in additional experiments using dioxane as the solvent. By measurements of the molar polarization, molar refraction, and density at different phloretin concentrations (data not shown) and extrapolation to infinite dilution (Hedestrand method), which corresponds to the gas phase, we estimated the dipole moment using the Debye and the Clausius-Mosotti equations (Exner 1975; Minkin et al. 1970). The determined value was 3.3 ± 0.5 D, which agrees very well with our calculated value for the gas phase (see Table 2).

Adsorption isotherm of phloretin to SSV

In this study we determined the adsorption of phloretin to lipid bilayers in a direct way, measuring the concentration of phloretin in buffer before and after adsorption

to SSVs. Solid supported bilayers (SSVs) (Bayerl and Bloom 1990) are suitable for this purpose since they can easily be separated by centrifugation and permit therefore, more than pure lipid vesicles (Verkman and Solomon 1982), an easy spectrophotometric determination of the concentration of phloretin in the aqueous phase. Phloretin in its undissociated form has an absorption peak at a wavelength of 285 nm. Figure 5A shows the adsorption isotherm of phloretin to egg-PC bilayers on a solid support dependent on the aqueous concentration of phloretin. Adsorption is given as the molar ratio of phloretin adsorbed to lipid. Adsorption of phloretin to monolayers and membranes is usually described by a Langmuir adsorption isotherm (De Levie et al. 1979;
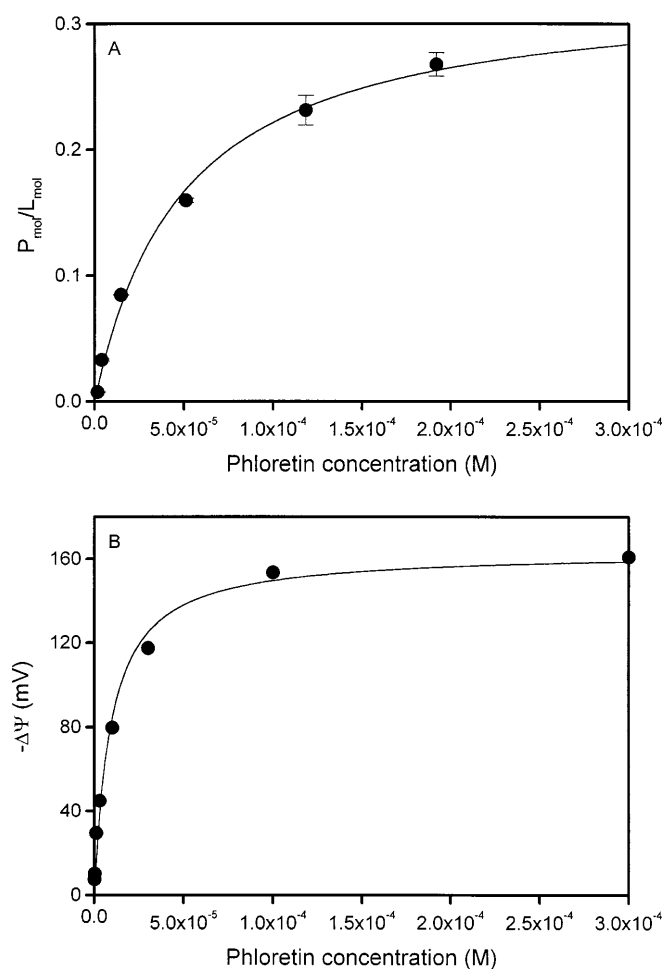
Fig. 5 A Adsorption of phloretin to egg-PC bilayers on a solid support denoted as the molar ratio of adsorbed phloretin/lipid, P_{mol}/L_{mol}, versus the aqueous phloretin concentration. The data are fitted according to the Langmuir adsorption isotherm (Eq. 3), where instead of the surface density, Γ, the molar ratio is used for the calculation. **B** Change of dipole potential, $\Delta\Psi$, of egg-PC black lipid membranes versus aqueous phloretin concentration obtained from charge-pulse experiments with the lipophilic ion dipicrylamine. The data were taken from Cseh and Benz (1998) and fitted according to Eq. (5). In both experiments the aqueous phase contained 100 mM NaCl and 20 mM NaH_2PO_4, the pH was 5.5, and the temperature was 22 °C. The standard deviations were below ± 10 mV. For details refer to the text

Reyes et al. 1983). This means that the surface density of adsorbed molecules, Γ, is dependent on the aqueous concentration, c, and converges to a saturation limit at high concentrations. The maximum surface density, Γ_∞, and the dissociation constant, k, are the characteristic parameters of the Langmuir adsorption isotherm:

$$\Gamma = \frac{\Gamma_\infty c}{c + k} \tag{3}$$

In a previous study we have demonstrated that Eq. (3) provides only an approximate first-order description of the adsorption of dipole molecules to surfaces because it neglects the important dipole-dipole interaction at the lipid surface. Nevertheless, it is possible to use the Langmuir fit as a first-order approximation. It yielded a maximum molar ratio of 0.3 (which corresponds to a maximum phloretin surface density, Γ, of approximately 43 μmol/m^2 as calculated from the surface area of the lipid on the SSV) and a dissociation constant, k, of 49 μM.

Another possible way to determine k is to refer to the dipole potential change, $\Delta\Psi$, which accompanies the adsorption of phloretin to lipid monolayers and bilayers (Andersen et al. 1976; Cseh and Benz 1998). The change in the dipole potential of monolayers and bilayers as a function of the surface density of adsorbed molecules bearing a dipole moment, such as phloretin, can be described as:

$$\Delta\Psi = \frac{4\pi\mu N_A \Gamma \sin\Theta}{\varepsilon} \tag{4}$$

wherein μ is the dipole moment of a single adsorbed molecule, Θ the angle between the direction of the dipole moment vector and the water/lipid interface, N_A Avogadro's number, and ε the effective dielectric constant in the dipole plane. Detailed descriptions of the adsorption model are given elsewhere (Cousin and Motais 1978; Cseh and Benz 1998; De Levie et al. 1979; Reyes et al. 1983). According to Eq. (4), $\Delta\Psi$ is a linear function of the dipole surface density; therefore the corresponding maximum surface density can be expressed by the maximum potential change, $\Delta\Psi_\infty$, which leads to:

$$\Delta\Psi = \frac{\Delta\Psi_\infty c}{c + k} \tag{5}$$

Figure 5B shows the dipole potential change of phloretin to egg-PC bilayers[1] dependent on the aqueous concentration of phloretin as taken from Cseh and Benz (1998). The fit according to Eq. (5) yielded a maximum potential change of 164 mV and a dissociation constant of 9 μM. Both values agree well with those that have

been found by Reyes et al. (1983) ($\Delta\Psi_\infty = 200$ mV, $k = 7$ μM).

With both methods it can be shown that the adsorption of phloretin saturates with increasing aqueous concentration and that the data can be fitted according to the Langmuir adsorption isotherm as a first-order approximation[2]. Independent of the different methods, the parameters of the Langmuir adsorption isotherm should correspond with one another. It is impossible to calculate the surface density of phloretin because of the unknown parameters that determine $\Delta\Psi$ (Eq. 4). Thus, we cannot compare the values of maximum adsorption, but it is possible to derive the dissociation constant, k, which represents a meaningful number for the affinity of phloretin to the lipid. The values of k derived from Fig. 5A and B, however, differ by a factor of about 5 using the two methods. Differences of the same order of magnitude were also found for experiments with phloretin analogs (data not shown). This considerable discrepancy cannot be explained by statistical dispersion of the experimental data alone, but must be caused by the functional relationship between the dipole potential determining parameters. The dipole potential change is related to the surface density according to Eq. (4), i.e. any variation of the involved parameters influences $\Delta\Psi$. A surface density dependent variation of one or more parameters in Eq. (4) might be an explanation of the different value of k determined by the dipole potential change measurements (Cseh and Benz 1998; see also Discussion).

^{2}H NMR with unilamellar lipid vesicles on a spherical support (SSV)

The adsorption of phloretin to membrane surfaces suggests that it interacts mainly with the phospholipid head groups (Bechinger and Seelig 1991; Cseh and Benz 1999). To study this possible interaction in more detail, we performed ^{2}H NMR measurements with phloretin and the head group deuterated lipid DMPC-d_{13}. Figure 6, lower panel, shows a comparison of the ^{2}H NMR spectra of DMPC-d_{13} SSVs without (dotted line) and with (solid line) 50 mol% phloretin. The upper panel of Fig. 6 demonstrates the corresponding depaked oriented spectra without (dotted line) and with (solid line) phloretin. When the motional freedom of the headgroup moieties is considered, it is possible to assign the quadrupolar splitting of 1025 Hz to the nine protons in the three methyl groups of choline for the spectrum without phloretin. Similarly, that of 5.6 kHz could be designated to the end segments of the head group, which

---

[1] The data are taken from Cseh and Benz (1998). The phloretin-induced change in dipole potential of black lipid bilayer membranes was estimated from its influence on dipicrylamine transport parameters in charge-pulse experiments described elsewhere (Benz and Cros 1978; Pickar and Benz 1978)

[2] We have shown recently (Cseh and Benz 1998) that the Langmuir fit according to Eq. (5) can be improved when we take into consideration that the dipole potential represents an additional driving force for the adsorption of dipolar molecules. According to the improved model, the fit of the data shown in Fig. 5B exhibited a $\Delta\Psi_\infty$ of 188 mV and a k of 4.31 μM. However, for the purpose in this section the accuracy of the fit in Fig. 5B is sufficient
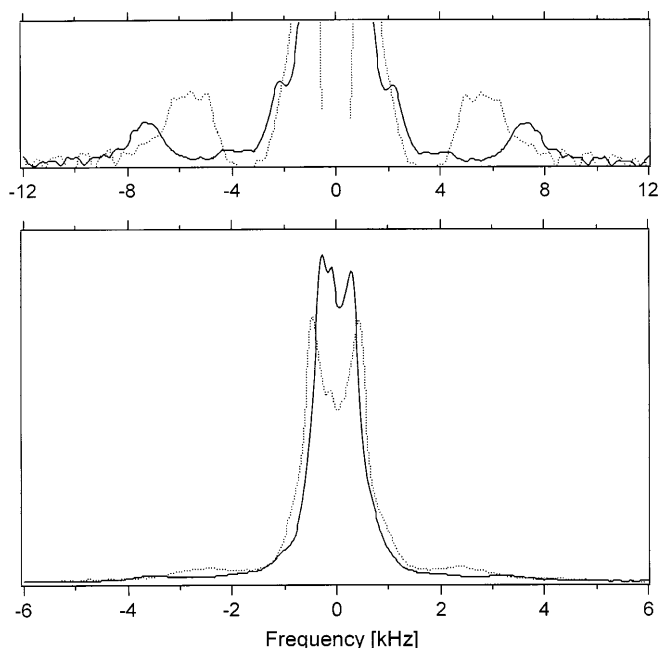
Fig. 6 ^{2}H NMR spectra of DMPC-d_{13} SSVs at 30 °C without (*dotted line*) and with (*solid line*) 50 mol% phloretin. *Bottom panel*: powder spectra. *Top panel*: calculated oriented spectra. The pulse spacing of the ^{2}H NMR spectra was 35 μs. The third (central) maximum of the deuterium methyl resonance in both the spectra with and without phloretin in the lower panel is probably caused by free deuterium in the suspension

could not be separated in the absence of phloretin. Phloretin has a considerable effect on the ^{2}H NMR spectra of DMPC-d_{13} SSVs. Its incorporation resulted in quadrupolar splittings of 733 Hz for the methyl groups and 7.3 and 2.2 kHz for the α and β methylenes, respectively. This result can be understood by simple geometrical considerations, if we assume that phloretin is indeed localized within the polar head groups. Similarly, the tendency of increased splitting for the α segment and decreased splitting for the β segment has previously been reported for 1-palmitoyl-2-oleoyl-3-phosphatidylcholine (POPC) multilamellar vesicles, when phloretin is present (Bechinger and Seelig 1991). Additionally, we measured a decrease of the splitting of the methyl groups, which is a result of the same effect. It has previously been reported for negatively charged molecules/amphiphiles that their addition to a lecithin bilayer changes the orientation of the $^-$P-N$^+$ dipole from nearly parallel to the membrane surface to an orientation more towards the hydrocarbon phase (Scherer and Seelig 1989). It is obvious that a similar

effect was here observed for the incorporation of phloretin in the SSV.

We measured spin-lattice relaxation of the choline headgroup to investigate the changes of the headgroup dynamics as a result of the incorporation of phloretin. The results of these experiments are summarized in Table 3. We found similar T_{1z} values without (23.2 ± 0.7 ms) and with (22.9 ± 0.3 ms) 50 mol% phloretin. T_{1z} is sensitive to fast motions in the Larmor frequency regime and therefore the results give no indication for an altered headgroup dynamics in the frequency range of the quadrupolar resonance when phloretin is present.

For curved bilayers, the dominating relaxation mechanism in NMR measurements is lateral diffusion of the phospholipids (Köchy and Bayerl 1993; Sternin et al. 1983) and the diffusion correlation time is defined by $t_D = R^2/6D$, where D is the lateral diffusion constant and R is the radius of the curvature. We investigated the transverse relaxation time T_{2e}, which has been shown to be sensitive to motions that are slow on the NMR time scale t_M (here $t_M = 1/\sqrt{M_{2r}} = 9.3 \times 10^{-5}$ s obtained from the residual second moment M_{2r} of the pure DMPC-d_{13} bilayer). In the slow motion limit of $t_D \gg t_M$ and for a separation t in the two-pulse echo experiment of $t \gg t_M$, the T_{2e} time is proportional to t_D (Pauls et al. 1985), i.e. a slower lateral diffusion would yield a slower transverse relaxation rate. In the fast motion limit $t_D \ll t_M$ the relaxation rate, $1/T_{2e}$, is proportional to the residual second moment M_{2r} (Pauls et al. 1985); thus an increased M_{2r} would lead to a faster transverse relaxation.

In our study we measured, for the pure DMPC-d_{13} SSVs $T_{2e} = 862 \pm 45$ μs and with phloretin $T_{2e} = 1402 \pm 18$ μs. Considering M_{2r} of all head group deuterons together the slow motion limit $t_D \gg t_M$ is fulfilled. This result could mean that phloretin reduced the lateral diffusion of the lipids. However, if we assume the methyl moieties to dominate the measured T_{2e} relaxation time, then their M_{2r} can be calculated according to $M_{2r} = 4\pi^2/5\Delta\nu_Q^2$, giving $t_M = 35 \times 10^{-5}$ s for the pure system and $t_M = 49 \times 10^{-5}$ s with phloretin. In our study we used silica beads as a solid support with a diameter of 400 nm. For pure DPPC multilayers a diffusion constant of $(12 \pm 1) \times 10^{-12}$ m^2/s has been reported (Karakatsanis and Bayerl 1996), which results in a diffusion correlation time $t_D = 55 \times 10^{-5}$ s. This means that for both t_M values neither the fast nor the slow motion limit strictly applies ($t_D = 55 \times 10^{-5}$ s) and thus the reduction in T_{2e} relaxation might be simply a result of the reduction in quadrupolar splitting and

Table 3 Results of ^{2}H NMR spectroscopy measurements from line shape and relaxation experiments on DMPC-d_{13} spherical supported unilamellar vesicles (SSVs) with and without 50 mol% phloretin at pH 7

SSV	CH$_3$ ν_Q (Hz)	T_1 (ms)	T_2 (μs)	M_{2r} ($10^8 \times$ 1/s^2)
Without phloretin	1025, 5600	23.2 ± 0.7	862 ± 45	1.18
With phloretin	733, 2198, 7255	22.9 ± 0.3	1402 ± 18	1.16

phloretin has a negligible influence on lipid diffusion along the silica beads.

Discussion

Interaction of phloretin with lipids in membranes

The results of the DSC measurements clearly demonstrated that phloretin decreases the phase transition temperature of lipid membranes. This effect is dependent on the concentration of its neutral form in the lipid phase and indicates that phloretin integrates into the membrane and changes the lipid packing (Biltonen and Lichtenberg 1993). However, a pure hydrophobic interaction between the lipid and phloretin, i.e. its simple integration into the hydrophobic interior of the membrane, cannot be supported by our DSC study. Despite the high degree of integration as judged by the strong decrease of the phase transition temperature, the endotherms show only weak broadening indicating that the cooperativity of lipid phase transition is hardly affected. In contrast to this, the integration of hydrophobic molecules into the hydrocarbon region of the lipid layer affects strongly the cooperativity of the phase transition and leads to a large broadening of the endotherms (Reinl and Bayerl 1993). This result agrees with lipid monolayer experiments on a Langmuir trough (Cseh and Benz 1999), where we have shown that phloretin affects lipid packing, but this effect is counterbalanced by increasing surface pressures, leading to a gradual squeezing out of phloretin at higher surface pressures, which are likely to exist in bilayers. Simultaneous monitoring of the dipole potential change, however, has demonstrated that phloretin remains adsorbed to the monolayer. Therefore, the interaction of phloretin with lipids seems to be restricted to that within the headgroups, which suggests that phloretin molecules integrated into the lipid layer are preferentially localized within the headgroup region. The DSC experiments with MLV described here confirm the monolayer results. Another indication of the preferential location of phloretin within the headgroups has been given by Bechinger and Seelig (1991). In their NMR study the order of the hydrocarbon chains in POPC membranes remains almost unaltered whereas the headgroup orientation is considerably changed by phloretin.

Phloretin conformers and their dipole moments

In a recent study we have shown that the adsorbed dipoles influence one another, when their density is large enough. As a consequence, the adsorption of dipole molecules does not follow any longer the Langmuir adsorption isotherm (Cseh and Benz 1998). It is also possible that the adsorbed dipoles have an influence on the conformation of the further adsorbed dipole molecules.

The calculation of the stable phloretin conformers revealed a wide distribution of possible dipole moments. We therefore cannot refer to phloretin as a molecule with a clearly defined dipole moment with respect to the effects on the dipole potential of monolayers and membranes. Neither we can proceed with the assumption that the conformers all show the same lipid affinity and behave as one single molecule. These aspects acquire some importance when we try to correlate the reduction of the dipole potential at the adsorption of phloretin with the size of its overall dipole moment. Reyes et al. (1983) have found in their study that the dipole moments of phloretin and its analogs roughly correlate with the dipole potential change, but they also have observed exceptions to this rule. They have concluded that the change in dipole potential is not a simple function of the dipole moment of the adsorbed molecule but is highly dependent on the number and position of the hydroxyl groups in the ring and the surface density in the membrane. Having in mind the large variation of the dipole moments of the phloretin conformers calculated here and their strong dependence on the orientation of the OH moieties, it is possible that the dipole moments of adsorbed molecules are different from the overall dipole moment of molecules in the aqueous phase and, moreover, they may indeed change their conformation when they adsorb to the lipid layer, thereby changing their dipole moment. Furthermore, the situation at the membrane-water interface could even be more complicated when we consider the possibility that the adsorption of phloretin to the membrane surface changes the amount of water and orientation of water dipoles associated with the lipid surface.

Parameters of phloretin adsorption to membranes

The results of our adsorption experiments with phloretin clearly demonstrated that a considerable problem exists when we consider the dissociation constants determined here and those obtained from dipole potential measurements. The critical difference between these two methods is that the latter one is only able to properly describe the adsorption of a dipole molecule if it is accompanied by a dipole potential change. Moreover, adsorption usually has been described using a static electrical model, which means that the relation between the surface density of phloretin molecules adsorbed to the lipid layer and the dipole potential change is supposed to be linear (De Levie et al. 1979; Reyes et al. 1983). However, this assumption is only valid when the parameters involved in Eq. (4) are taken as constants and do not depend on the surface density or on the dipole potential change. Recently, we have demonstrated that the dipole potential of a membrane represents a considerable driving force for the adsorption of a dipolar molecule to the membrane (Cseh and Benz 1998). This means that the entire driving force for adsorption of such a molecule can be split into a part that represents the Langmuir interaction and a part which is

dependent on the existing dipole potential of a membrane and therefore decreases with the decrease of total dipole potential of the lipid layer. The observed difference between the dissociation constants derived from the dipole potential change and the adsorption of phloretin to the SSV can be explained if we take into account the relation between the dipole potential as a driving force and the alignment of the adsorbed dipoles as its effect. If we assume that the dipoles of the adsorbed molecules can change their direction and their dipole moment, they will respond to the preexisting potential with uniform alignment opposite to the electric field and therefore decrease the dipole potential of membranes and monolayers. Consequently, at a certain surface density of adsorbed molecules the total dipole potential of the lipid layer will reach a very small value close to that where the dipoles of further adsorbed phloretin molecules will be randomly aligned and do not contribute to $\Delta\Psi$ any more. This means that the change of dipole potential caused by the adsorption of phloretin to membranes strictly depends on the preexisting potential. Our adsorption model previously proposed (Cseh and Benz 1998) takes account of this by separating the Langmuir and the dipole-dipole interaction. Following this approach, we conclude that even if the value of $\Delta\Psi$ is close to the maximum value $\Delta\Psi_\infty$ and saturates at a given phloretin concentration, a further adsorption according to the Langmuir interaction may still be possible. As a consequence, the dissociation constant calculated from the change of the dipole potential and from the direct adsorption experiments differ considerably, as shown here. Furthermore, we have to conclude that adsorption isotherms obtained from measurements of the dipole potential change are able to describe the electrical aspects of adsorption of a dipole molecule to lipid membranes. However, they do not allow a proper description of their adsorption at high surface density if it is no longer accompanied by a change of dipole potential. This means that the dipole moments of adsorbed phloretin molecules must not be regarded as static quantities because of the heterogeneous dipole moment distribution of the various conformers; they may change, dependent on their surface density. Our theoretical calculations demonstrate that this is indeed possible.

Verkman and Solomon (1982) have investigated the permeation of phloretin through lipid bilayers and found in their study that although the binding of phloretin to a lipid membrane is a saturable process, the permeation kinetics appear to be unsaturable. The same result has recently been reported by Pohl et al. (1997). Verkman and Solomon (1982) have suggested two binding sites with different affinities for phloretin to account for this phenomenon. Pohl et al. (1997) have proposed that phloretin adsorption and transmembrane permeation should be considered as competitive events. This means that prior to phloretin permeation, no adsorption to the interface is required. They assumed that in contrast to adsorbed phloretin, which reduces the dipole potential, diffusing phloretin is randomly aligned and therefore not detectable by means of dipole potential measurements. However, although we neither found indications of multiple binding sites on the basics of our own adsorption measurements nor favor a model which treats adsorption and permeation as processes that are independent of each other, it seems reasonable to distinguish different states of phloretin at the water-lipid interface, in particular at high surface densities when the phloretin-mediated dipole potential decrease of the lipid layer is considerable. This means that the dipole moments normal to the interface of adsorbed phloretin molecules may differ from each other. Phloretin conformers with different dipole moments, as is suggested by our computational conformational analysis of phloretin, may well account for the discrepancies between adsorption and permeation that have been described previously (Pohl et al. 1997; Verkman and Solomon 1982).

References

Andersen OS, Finkelstein A, Katz I, Cass A (1976) Effect of phloretin on the permeability of thin lipid membranes. J Gen Physiol 67: 749–771

Bayerl TM, Schmidt CF, Sackmann E (1988) Kinetics of symmetric and asymmetric phospholipid transfer between small sonicated vesicles studied by DSC, electron microscopy and dynamic light scattering. Biochemistry 27: 6078–6085

Bayerl TM, Bloom M (1990) Physical properties of single phospholipid bilayers adsorbed to micro glass beads. A new vesicular model system studied by ^{2}H-nuclear magnetic resonance. Biophys J 58: 357–362

Bechinger B, Seelig J (1991) Interaction of electric dipoles with phospholipid head groups. A ^{2}H and ^{31}P NMR study of phloretin analogues in phosphatidylcholine membranes. Biochemistry 30: 3923–3929

Ben-Yashar V, Menashe M, Biltonen RL, Johnson M, Barenholz Y (1987) Interaction of transparinaric acid with phosphatidylcholine bilayers: comparison with the effects of other fluorophores. Biochim Biophys Acta 904: 117–124

Benz R, Cros D (1978) Influence of sterols on ion transport through lipid bilayer membranes. Biochim Biophys Acta 506: 265–280

Biltonen RL, Lichtenberg D (1993) The use of differential scanning calorimetry as a tool to characterize liposome preparations. Chem Phys Lipids 64: 129–142

Cevec G, Watts A, Marsh D (1981) Titration of phosphatidylserine bilayer membranes. Effects of pH, surface electrostatics, ion binding, and head-group hydration. Biochemistry 20: 4955–4965

Cousin JL, Motais R (1978) Effect of phloretin on chloride permeability: a structure-activity study. Biochim Biophys Acta 507: 531–538

Cseh R, Benz R (1998) The adsorption of phloretin to lipid monolayers and bilayers cannot be explained by Langmuir adsorption isotherms alone. Biophys J 74: 1399–1408

Cseh R, Benz R (1999) Interaction of phloretin with lipid monolayers: relationship between structural changes and dipole potential change. Biophys J 77: 1477–1488

De Levie R, Rangarajan SK, Seelig PF, Andersen OS (1979) On the adsorption of phloretin onto a black lipid membrane. Biophys J 25: 295–300

Dewar MJS, Zoebisch EG, Healey EF, Stewart JJP (1985) AM1: A new general purpose quantum mechanical molecular model. J Am Chem Soc 107: 3902–3909

Exner O (1975) Dipole moments in organic chemistry. Thieme, Stuttgart

Forman SA, Verkman AS, Dix JA, Solomon AK (1982) Interaction of phloretin with the anion transport protein of the red blood cell membrane. Biochim Biophys Acta 689: 531–538

Frisch MJ, Trucks GW, Schlegel HB, Gill PMW, Johnson BG, Robb MA, Cheeseman JR, Keith TA, Petersson GA, Montgomery JA, Raghavachari K, Al-Laham MA, Zakrzewski VG, Ortiz JV, Foresman JB, Cioslowski J, Stefanov BB, Nanayakkara A, Challacombe M, Peng CY, Ayala PY, Chen W, Wong MW, Andres JL, Replogle ES, Gomperts R, Martin RL, Fox DJ, Binkley JS, Defrees DJ, Baker J, Stewart JP, Head-Gordon M, Gonzalez C, Pople JA (1995) Gaussian 94 (revision F.1). Gaussian, Pittsburgh

Gunn RB, Wieth JO, Tosteson DC (1975) Some effects of low pH on chloride exchange in human red blood cells. J Gen Physiol 65: 731–749

Hawkins GD, Giesen DJ, Lynch GC, Chambers CC, Rossi I, Storer JW, Rinaldi D, Liotard DA, Cramer CJ, Truhlar DG (1997) AMSOL version 6.1.1. University of Minnesota, Minneapolis (based in part on AMPAC version 2.1 by Liotard DA, Healy EF, Ruiz JM, Dewar MJS and on the EF routines by Jensen F)

Heise H, Bayerl TM, Isenberg G, Sackmann E (1991) Human platelet P-235, a talin-like actin binding protein, binds selectively to mixed lipid bilayers. Biochim Biophys Acta 1061: 121–131

Jacobson K, Papahadjopoulos D (1975) Phase transitions and phase separations in phospholipid membranes induced by changes in temperature, pH, and concentration of bivalent cations. Biochemistry 14: 152–161

Jennings ML, Solomon AK (1976) Interaction between phloretin and the red cell membrane. J Gen Physiol 67: 381–397

Karakatsanis P, Bayerl TM (1996) Diffusion measurements in oriented phospholipid bilayers by proton-NMR in a static fringe-field gradient. Phys Rev E 54: 1785–1790

Kodama M, Kuwabara M, Seki S (1982) Successive phase-transition phenomena and phase-diagram of the phosphatidylcholine-water system as revealed by differential scanning calorimetry. Biochim Biophys Acta 389: 567–572

Köchy T, Bayerl TM (1993) Lateral diffusion-coefficients of phospholipids in spherical bilayers on a solid support measured by ^{2}H-nuclear-magnetic-resonance relaxation. Phys Rev E 47: 2109–2116

Kurrle A, Rieber P, Sackmann E (1990) Reconstitution of transferrin receptor in mixed lipid vesicles. An example of the role of elastic and electrostatic forces for protein/lipid assembly. Biochemistry 29: 8274–8282

Lee AG (1977) Lipid phase transitions and phase diagrams. Biochim Biophys Acta 472: 237–281

LeFevre PG, Marshall JK (1959) The attachment of phloretin and analogues to human erythrocytes in connection with inhibition of sugar transport. J Biol Chem 234: 3022–3026

Linseisen FM, Thewalt JL, Bloom M, Bayerl TM (1993) ^{2}H-NMR and DSC study of SEPC-cholesterol mixtures. Chem Phys Lipids 65: 141–149

Lohner K, Schuster A, Degovics G, Muller K, Laggner P (1987) Thermal phase behaviour and structure of hydrated mixtures between dipalmitoyl- and dihexadecylphosphatidylcholine. Chem Phys Lipids 44: 61–70

Macey RJ, Farmer REL (1970) Inhibition of water and solute permeability in human red cells. Biochim Biophys Acta 211: 104–106

McElhaney RN (1982) The use of differential scanning calorimetry and differential thermal analysis in studies of model and biological membranes. Chem Phys Lipids 30: 229–259

Melnik E, Latorre R, Hall JE, Tosteson DC (1977) Phloretin-induced changes in ion transport across lipid bilayer membranes. J Gen Physiol 69: 243–247

Minkin VI, Osipov OA, Zhdanov YA (1970) Dipole moments in organic chemistry (English translation). Plenum Press, New York

Naumann C, Brumm T, Bayerl TM (1992) Phase-transition behavior of single phosphatidylcholine bilayers on a solid spherical support studied by DSC, NMR and FT-IR. Biophys J 63: 1314–1319

Osdol WW van, Ye Q, Johnson ML, Biltonen RL (1992) Effects of the anesthetic dibucaine on the kinetics of the gel-liquid crystalline transition of dipalmitoylphosphatidylcholine multilamellar vesicles. Biophys J 63: 1011–1017

Owen JD (1974) The effect of phloretin on the potassium conductance in *Aplysia* giant neurons. J Membr Biol 16: 65–78

Pauls KP, MacKay AL, Söderman O, Bloom M, Tanjea AK, Hodges RS (1985) Dynamic properties of the backbone of an integral membrane polypeptide measured by ^{2}H-NMR. Eur Biophys J 12: 1–11

Pickar AD, Benz R (1978) Transport of oppositely charged lipophilic probe ions in lipid bilayer membranes having various structures. J Membr Biol 44: 353–376

Pohl P, Rokitskaya TI, Pohl EE, Saparov SM (1997) Permeation of phloretin across bilayer lipid membranes monitored by dipole potential and microelectrode measurements. Biochim Biophys Acta 1323: 163–172

Rauhut G, Chandrasekhar J, Alex A, Beck B, Sauer W, Clark T (1998) VAMP 6.1. Oxford Molecular

Reinl HM, Bayerl TM (1993) Interaction of myelin basic protein with single bilayers on a solid support: an NMR, DSC and polarized infrared ATR study. Biochim Biophys Acta 1151: 127–136

Reyes J, Greco F, Motais R, Latorre R (1983) Phloretin and phloretin analogs: mode of action in planar lipid bilayers and monolayers. J Membr Biol 72: 93–103

Scherer PG, Seelig J (1989) Electric charge effects on phospholipid headgroups. Phosphatidylcholine in mixtures with cationic and anionic amphiphiles. Biochemistry 28: 7720–7728

Sternin E, Bloom M, MacKay AL (1983) De-pake-ing of NMR spectra. J Magn Reson 55: 274–282

Stewart JJP (1989) Optimization of parameters for semiempirical methods II. applications. J Comput Chem 10: 221–264

SYBYL 6.5 (1999) Tripos Associates, St. Louis

Toon MR, Solomon AK (1987) Modulation of water and urea transport in human red cells: effects of pH and phloretin. J Membr Biol 99: 157–164

Verkman AS, Solomon AK (1982) A stepwise mechanism for the permeation of phloretin through a lipid bilayer. J Gen Physiol 80: 557–581